Ionics (2014) 20:145–149
DOI 10.1007/s11581-013-1017-8

SHORT COMMUNICATION

# Composites of olive-like manganese oxalate on graphene sheets for supercapacitor electrodes

**Tingting Liu · Guangjie Shao · Mingtong Ji · Zhipeng Ma**

Received: 10 June 2013 / Revised: 3 October 2013 / Accepted: 23 October 2013 / Published online: 12 November 2013


**Abstract** $MnC_2O_4$/graphene composites are prepared by a facile hydrothermal reaction with $KMnO_4$ using ascorbic acid as a reducing agent. Olive-like $MnC_2O_4$ particles are distributed uniformly on the surface of graphene sheets. The composites are evaluated as supercapacitor electrodes, which show that the specific capacitance of $MnC_2O_4$/graphene composites is 122 F $g^{-1}$, more than twice as high as that of free $MnC_2O_4$ at a current density of 0.5 A $g^{-1}$. In addition, this composite material exhibits an excellent cycle stability with the capacitance retention of 94.3 % after 1,000 cycles.

**Keywords** Supercapacitor · Hydrothermal · Graphene · Manganese oxalate · Composites

## Introduction

The increasing demand for clean and sustainable energy has driven intensive researches toward the development of energy storage devices. Supercapacitors have attracted much attention due to their excellent properties, such as high power density, long cycle life, and fast charge–discharge rates [1–3].

Recently, the development of graphene-based materials for application as supercapacitive materials attracts much attention. Graphene, a carbon material with one-atom-thick layer 2D structure, exhibits a potential application for establishing a mixed conducting network to improve electrochemical performance of pseudocapacitive materials such as $Co_3O_4$ [4, 5], $MnO_2$ [6, 7], and NiO [8, 9], due to its extraordinary electrical and chemical stability and high surface-to-volume ratio. Moreover, the interleaved network of graphene can hinder the agglomeration of metal oxides dispersed on the surface of graphene. Importantly, the results obtained from these composite materials as supercapacitive materials demonstrate that graphene can enhance the capacitance and rate capability of metal oxides electrodes efficiently.

Anhydrous or hydrated manganese (II) oxalates are widely used as the precursors to produce nanoparticles of manganese oxides, which have extensive applications in the fields of magnetic materials, sorbents, and catalyst. Ahmad et al. [10] reported that the manganese oxalate precursor was used to synthesize single-phase nanoparticles of various manganese oxides such as MnO, $Mn_2O_3$, and $Mn_3O_4$ under specific reaction conditions. In addition, Nikumbh [11] studied on thermal and electrical properties of manganese oxalate dehydrate, indicating that the final products of decomposition in static air and dynamic air were $Mn_3O_4$ for $MnC_2O_4 \cdot 2H_2O$.

Despite the physical and chemical properties of manganese oxalates have been widely researched, electrochemical performance of this metal oxalate compound is rarely reported. Herein, we report a facile approach to prepare olive-like $MnC_2O_4$ particles by a hydrothermal reaction from $KMnO_4$, using ascorbic acid (AA) as a reducing agent. Moreover, to enhance the capacitance of $MnC_2O_4$, the particles are dispersed on the surface of graphene sheets. The supercapacitive properties of the as-prepared $MnC_2O_4$/graphene composite are discussed in this paper, which shows greatly potential performance.

## Experimental

### Synthesis of samples

All the reagents used in the work were of analytical grade. Graphene oxide (GO) was prepared from graphite powder by the modified Hummers method [12]. An appropriate amount

T. Liu · G. Shao (✉) · Z. Ma
Hebei Key Laboratory of Applied Chemistry, College of Environmental and Chemical Engineering, Yanshan University, Qinhuangdao 066004, China
e-mail: shaoguangjie@ysu.edu.cn

T. Liu · M. Ji
Northeast Petroleum University at Qinhuangdao, Qinhuangdao 066004, China

of GO was treated upon microwave irradiation to obtain graphene. The microwave oven (Galanz WD900B) was first operated at the power of 720 W, 2,450 MHz for 60 s, and then 60 s at the power of 540 W. During this process, microwave assisted exfoliation and reduction of GO, which avoided using toxic hydrazine hydrate; 0.02 g graphene was dispersed in 20 mL of deionized water, and then, 0.2 g $KMnO_4$ was added into this suspension. Subsequently, 0.2 g AA was dispersed in 20 mL of deionized water and then added into the above solution under continuous stirring. The suspension was then transferred to a Teflon-lined autoclave and heated at 120 °C for 12 h. Finally, the precipitate was separated by centrifugation and then washed and dried. For comparison, free $MnC_2O_4$ was also prepared with the same procedure as described above in the absence of graphene.

### Materials characterization

X-ray diffraction (XRD) patterns were conducted on the D/Max-2500/PC X-ray diffractometer (Rigaku, Japan) with Cu Kα radiation ($\lambda = 0.15406$ nm) under a voltage of 40 kV and a current of 100 mA. Raman spectrum was recorded with the Raman Station 400F (Perkin-Elmer). Morphologies of the samples were studied with scanning electron microscopy (SEM) (S-4800, Hitachi, Japan). Thermogravimetric analysis (TGA) was performed with the DTG-60A thermal analysis system (Shimadzu, Japan) from 30 to 900 °C at a heating rate of 10 °C $min^{-1}$ under air atmosphere.

### Preparation of electrodes

Working electrodes were fabricated as follows [13]: firstly, the as-prepared electrode material, acetylene black, and poly(tetrafluoroethylene) (PTFE) were mixed in a weight ratio of 80:15:5, and absolute alcohol was used as the solvent to form a homogeneous paste. Acetylene black and PTFE were used as the conductive agent and binder, respectively. Then, the mixture was pressed into the nickel foam (1.0 cm × 1.0 cm) under a pressure of 2.0 MPa. Finally, the fabricated electrodes were dried at 60 °C for 12 h in a vacuum oven.

### Electrochemical measurements

Electrochemical measurements were performed under a three-electrode system. The $MnC_2O_4$/graphene composite, activated carbon, and Hg/HgO were used as the working, counter, and reference electrodes, respectively; 6 M KOH aqueous solution was used as the electrolyte. All the tests were conducted at ambient temperature. Galvanostatic charge/discharge curves were carried out using the NEware autocycler in the potential range from −0.1 to 0.55 V. Cyclic voltammetry (CV) and electrochemical impedance spectroscopy (EIS) were performed on the CHI 660A electrochemical workstation. CV tests were measured between −0.1 and 0.55 V, and EIS measurement was conducted in the frequency range from 100 kHz to 0.01 Hz at the open circuit potential with the amplitude of 5 mV.

## Results and discussion

Ascorbic acid may reduce $MnO_4^-$ at ambient temperature; however, the product is $MnO_2$ [14]. Under the hydrothermal condition, $MnO_4^-$ will be reduced further. In the end, $MnC_2O_4$ is generated at appropriate temperature and pressure. Consequently, the nanostructure of the product changes with the reaction condition.

The morphology of the as-prepared material is shown in Fig. 1. Figure 1a, b shows SEM images at different magnifications. The SEM image of $MnC_2O_4$/graphene composite shows that graphene sheets possess a nanoporous structure with wrinkled and transparent carbon nanosheets, which enables efficient transport of electrons and ions. Moreover, manganese oxalate particles with olive-like morphology can be observed clearly, which are distributed uniformly on the surface of graphene sheets. Interestingly, Fig. 1b indicates that manganese oxalate particles can be wrapped by graphene sheets.

Figure 2a shows the XRD pattern of the composite, which reveals that the major phase of this composite material corresponds to crystalline $MnC_2O_4 \cdot 2H_2O$ (JCPDS 25-0544), and the sharp peaks indicate good crystallinity. The interatomic distance of $MnC_2O_4 \cdot 2H_2O$ of the (112), (−131), (−402) and (200) are 2.661, 1.842, 2.998, and 4.715 Å, respectively. The crystalline size in the (112) diffraction of $MnC_2O_4$ particles within the composite material estimated according to the Debye–Scherrer equation is 55.56 nm. Raman spectrum of $MnC_2O_4$/graphene composite is shown in Fig. 2b. Characteristic bands of D and G from graphene are observed. The D band near 1,330 $cm^{-1}$ represents the breathing mode of $\kappa$-point phonons of $A_{1g}$ symmetry, which is caused by the defects and disorder in the hexagonal graphitic layers. The G band near 1,590 $cm^{-1}$ represents the in-plane vibration of the $sp^2$ carbon atoms (the $E_{2g}$ phonons) [15]. A broad 2D band near 2,650 $cm^{-1}$ is visible, owing to phonons scattering at zone boundary. Besides the carbon peaks, some minor peaks between 300 and 700 $cm^{-1}$ are attributed to $MnC_2O_4$. The intensity ratio of D band and G band ($I_D/I_G$) is 1.40. The relatively high value indicates the existence of many carbon disorders or defects, which could be useful to store an extra number of electrons [16].

TG-DTA curves were used to analyze the thermal behaviors of the composite (Fig. 3a). In general, the TGA curve shows two-step weight loss process. The first step indicates a 15 % weight loss upon heating from 30 to 150 °C, which is accompanied by a sharp endothermic peak at approximately

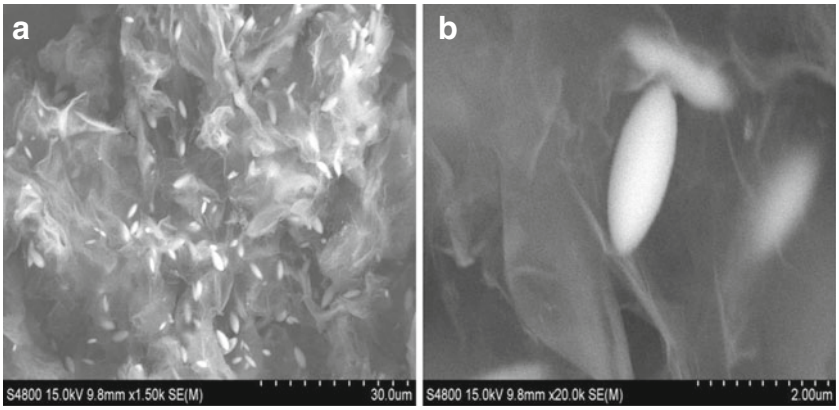


**Fig. 1** SEM images of the composite

150 °C, indicating the removal of crystal water. Subsequently, a weight loss about 35 % occurs in the temperature range of 280 to 400 °C. A sharp exothermic peak at 300 °C is attributed to the decomposition of $MnC_2O_4$ into $Mn_2O_3$ in the air, and a broad exothermic peak is observed at 350 °C, corresponding to the oxidation of graphene into $CO_2$ then escaped from the system [17]. Then, the weight is tending towards stability until 900 °C. The residues are mainly composed of $Mn_2O_3$. The mass ratio of $MnC_2O_4$ to graphene in the composite estimated from the TGA curves (Fig. 3b) is 96:4.

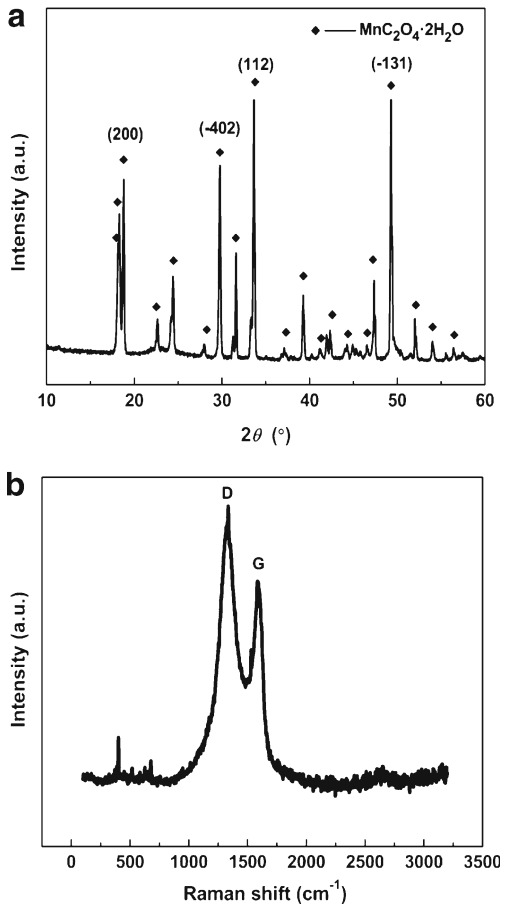


**Fig. 2** **a** XRD patterns of the composite. **b** Raman spectrum of the composite

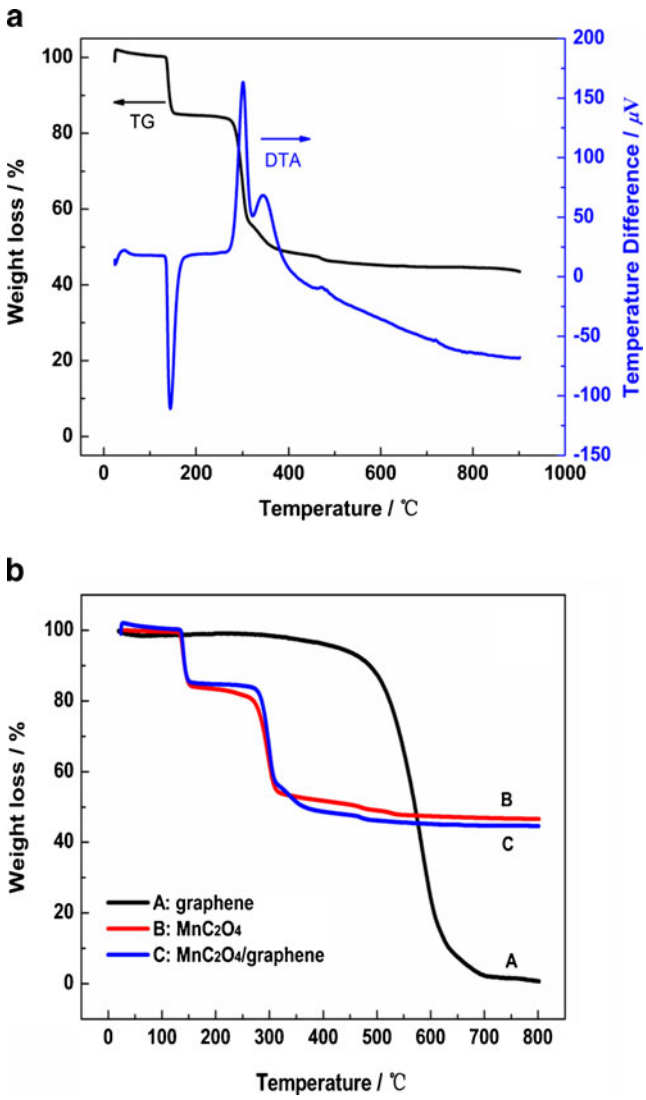


**Fig. 3** **a** TG-DTA curves of the composite. **b** TGA curves of graphene, $MnC_2O_4$, and $MnC_2O_4$/graphene composite

The electrochemical properties of $MnC_2O_4$/graphene composite were further evaluated. Figure 4a illustrates CV curves of the composite in 6 M KOH electrolyte at various scan rates from 2 to 50 mV $s^{-1}$. One pair of redox peaks is observed, corresponding to the redox reaction of $Mn^{2+}$/MnOOH, which indicates that the composite has a pseudocapacitance capability. Figure 4b shows galvanostatic charge–discharge curves of $MnC_2O_4$ and $MnC_2O_4$/graphene composite at a current density of 0.5 A $g^{-1}$. Both the charge–discharge curves show an approximately linear and symmetric triangular shape, which suggests good capacitive performance and reversible Faradic reaction. The charge–discharge efficiency of the composite obtained from the curve is 89.2 %. The increase of the discharge time indicates the higher capacitance of the composite than free $MnC_2O_4$. The specific capacitance could be calculated according the following formula:

$$C_{sp} = \frac{i \cdot t}{m \cdot \Delta V} \quad (1)$$

where $i$ is the constant current (ampere), $t$ is discharge time (second), $m$ is mass of active material, and $\Delta V$ is total potential deviation (volt). The specific capacitance of the composite is 122 F $g^{-1}$ (based on the overall mass), which is more than twice as high as that of free $MnC_2O_4$ (53 F $g^{-1}$). The value is comparable to composites of other manganese oxides combined with graphene, such as $Mn_3O_4$ and MnOOH [18, 19]. It could be attributed to the synergistic effect of $MnC_2O_4$ and graphene. Wrinkled graphene sheets overlapped with each other and formed a lot of pores, which will provide effective diffusion channels for electrolyte ions ($OH^-$). Moreover, graphene sheets served as substrates in the composites have offered an excellent electrical conductivity [20]. According to the preceding analysis, the mass content of graphene in the composite is so low, but the specific capacitance of the composite has been greatly improved. So, there is still a great potential for its future development. Nyquist plots of the composite are shown in Fig. 4c. The equivalent circuit of EIS is given in the inset of Fig. 4c, where $R_s$ is the solution resistance, $C_{dl}$ is the double layer capacitance, $R_{ct}$ is the charge transfer resistance, $Z_w$ represents the Warburg resistance, and $C_L$ is the limit capacitance. The internal resistance represented by the $x$-intercept is very small, approximately 0.6 Ω. The semicircle at the high-frequency region is also inconspicuous, which means that charge transfer resistance between the electrode surface and electrolyte is lower. Additionally, the line at the low-frequency region of the composite is almost vertical, indicating an ideal capacitive behavior [21].

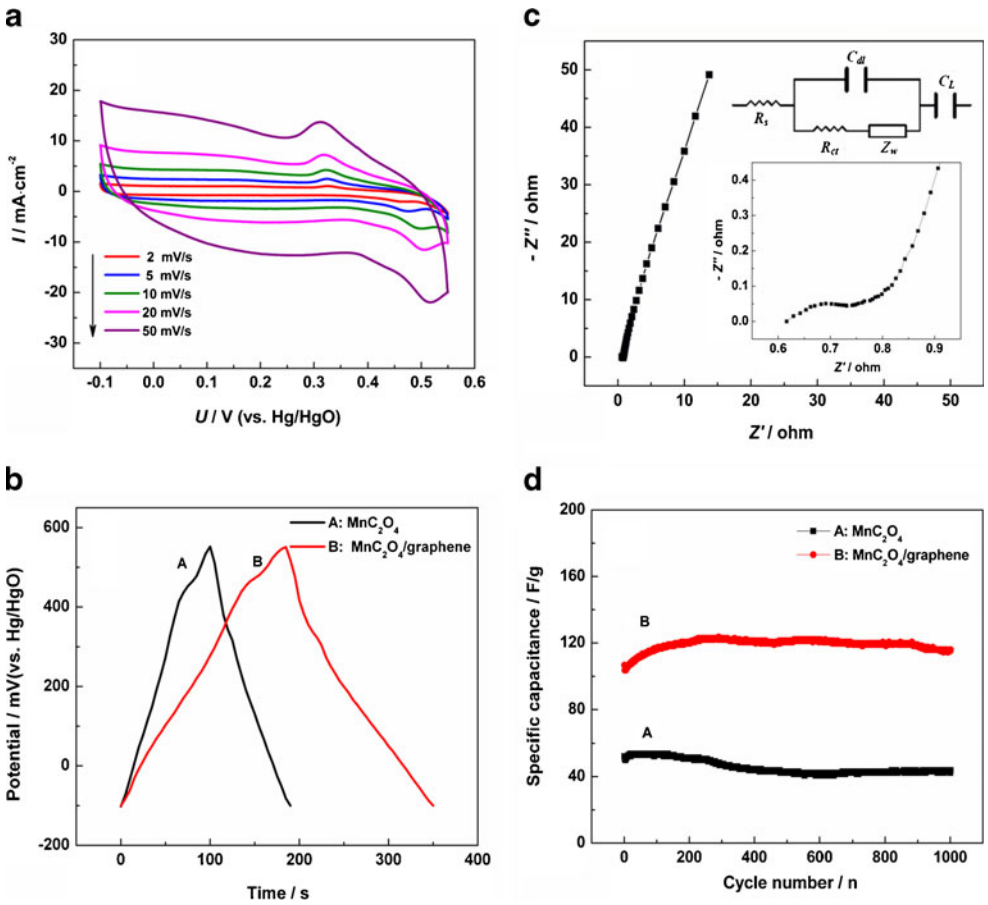


**Fig. 4** **a** Cyclic voltammograms of the composite at various scan rates. **b** Galvanostatic charge–discharge curves of $MnC_2O_4$ and the composite at a current density of 0.5 A $g^{-1}$. **c** Nyquist plots of the EIS for the composite. The *inset* shows the impedance spectrum of the initial state and the equivalent circuit. **d** Cycle stability of $MnC_2O_4$ and the composite electrode at a current density of 0.5 A $g^{-1}$ over 1,000 cycles

The cycle stability of the composite is examined at a current density of 0.5 A $g^{-1}$ over 1,000 cycles. As shown in Fig. 4d, the specific capacitance of the $MnC_2O_4$/graphene composite has an increase of about 15 % at the first 300 cycles (from 106 to 122 F $g^{-1}$). Even after 1,000 cycles, the composite still maintains 94.3 % of its maximum value (from 122 · to 115 F $g^{-1}$), which is better than free $MnC_2O_4$ (81.1 %, from 53 · to 43 F $g^{-1}$). The better stability of the composite is due to fact that graphene sheets with high conductivity have promoted fast Faradaic charge and discharge of manganese oxalate particles. Additionally, the initial increase of capacitance could be explained that active materials have not been fully utilized at the initial stage. After repetitive charge–discharge cycling, the active sites inside the nickel foam are fully exposed to the electrolyte [13].

## Conclusions

In summary, we synthesized composites of manganese oxalate on graphene sheets by a mild method. $MnC_2O_4$ has olive-like morphology and is distributed uniformly on the surface of graphene sheets. For the study of their application in supercapacitors as electrode materials, the $MnC_2O_4$/graphene composite exhibits higher capacitance and longer cycle life than free $MnC_2O_4$. It is due to the special structure of the composite and synergistic effects between manganese oxalate and graphene. The results have laid the foundation for our further study based on manganese oxalate. Simultaneously, it would be promising for the development of manganese compounds besides usual manganese oxides as electrode materials for supercapacitors.

**Acknowledgments** We are grateful for the financial support from the Natural Science Foundation of Hebei Province (B2012203069) and the Education Department of Hebei Province on Natural Science Research Key Projects for Institution of Higher Learning (ZH2011228).

## References

1. Miller JR, Simon P (2008) Electrochemical capacitors for energy management. Science 321:651–652
2. Simon P, Gogotsi Y (2008) Materials for electrochemical capacitors. Nat Mater 7:845–854
3. Liu C, Li F, Ma LP, Cheng HM (2010) Advanced materials for energy storage. Adv Mater 22:E28–E62
4. Xiang C, Li M, Zhi M, Manivannan A, Wu N (2013) A reduced graphene oxide/$Co_3O_4$ composite for supercapacitor electrode. J Power Sources 226:65–70
5. Zhou W, Liu J, Chen T, Tan KS, Jia X, Luo Z, Cong C, Yang H, Li CM, Yu T (2011) Fabrication of $Co_3O_4$-reduced graphene oxide scrolls for high-performance supercapacitor electrodes. Phys Chem Chem Phys 13:14462–14465
6. Zhao YQ, Zhao DD, Tang PY, Wang YM, Xu CL, Li HL (2012) $MnO_2$/graphene/nickel foam composite as high performance supercapacitor electrode via a facile electrochemical deposition strategy. Mater Lett 76:127–130
7. Chen S, Zhu J, Wu X, Han Q, Wang X (2010) Graphene oxide-$MnO_2$ nanocomposites for supercapacitors. ACS Nano 4:2822–2830
8. Cao X, Shi Y, Shi W, Lu G, Huang X, Yan Q, Zhang Q, Zhang H (2011) Preparation of novel 3D graphene networks for supercapacitor applications. Small 7:3163–3168
9. Inamdar AI, Kim Y, Pawar SM, Kim JH, Im H, Kim H (2011) Chemically grown, porous, nickel oxide thin-film for electrochemical supercapacitors. J Power Sources 196:2393–2397
10. Ahmad T, Ramanujachary KV, Lofland SE, Ganguli AK (2004) Nanorods of manganese oxalate: a single source precursor to different manganese oxide nanoparticles (MnO, $Mn_2O_3$, $Mn_3O_4$). J Mater Chem 14:3406–3410
11. Nikumbh AK, Athare AE, Pardeshi SK (1999) Thermal and electrical properties of manganese (II) oxalate dihydrate and cadmium (II) oxalate monohydrate. Thermochim Acta 326:187–192
12. Hummers WS, Offeman RE (1958) Preparation of graphitic oxide. J Am Chem Soc 80:1339
13. Gao Z, Wang J, Li Z, Yang W, Wang B, Hou M, He Y, Liu Q, Mann T, Yang P, Zhang M, Liu L (2011) Graphene nanosheet/$Ni^{2+}$/$Al^{3+}$ layered double-hydroxide composite as a novel electrode for a supercapacitor. Chem Mater 23:3509–3516
14. Wang YT, Lu AH, Zhang HL, Li WC (2011) Synthesis of nanostructured mesoporous manganese oxides with three-dimensional frameworks and their application in supercapacitors. J Phys Chem C 115: 5413–5421
15. Perera SD, Mariano RG, Nijem N, Chabal Y, Ferraris JP, Balkus KJ (2012) Alkaline deoxygenated graphene oxide for supercapacitor applications: an effective green alternative for chemically reduced graphene. J Power Sources 215:1–10
16. Zou Y, Kan J, Wang Y (2011) $Fe_2O_3$-graphene rice-on-sheet nanocomposite for high and fast lithium ion storage. J Phys Chem C 115: 20747–20753
17. Wang JG, Yang Y, Huang ZH, Kang F (2013) Effect of temperature on the pseudo-capacitive behavior of freestanding $MnO_2$@ carbon nanofibers composites electrodes in mild electrolyte. J Power Sources 224:86–92
18. Lee JW, Hall AS, Kim JD, Mallouk TE (2012) A facile and template-free hydrothermal synthesis of $Mn_3O_4$ nanorods on graphene sheets for supercapacitor electrodes with long cycle stability. Chem Mater 24:1158–1164
19. Wang L, Wang DL (2011) Preparation and electrochemical characterization of MnOOH nanowire-graphene oxide. Electrochim Acta 56:5010–5015
20. Yan J, Fan Z, Sun W, Ning G, Wei T, Zhang Q, Zhang R, Zhi L, Wei F (2012) Advanced asymmetric supercapacitors based on $Ni(OH)_2$/graphene and porous graphene electrodes with high energy density. Adv Funct Mater 22:2632–2641
21. Fan Z, Yan J, Wei T, Zhi L, Ning G, Li T, Wei F (2011) Asymmetric supercapacitors based on graphene/$MnO_2$ and activated carbon nanofiber electrodes with high power and energy density. Adv Funct Mater 21:2366–2375